THE JOURNAL OF BIOLOGICAL CHEMISTRY
Vol. 277, No. 43, Issue of October 25, pp. 40919–40929, 2002

Printed in U.S.A.

Localization *Versus* Function of Rab3 Proteins

EVIDENCE FOR A COMMON REGULATORY ROLE IN CONTROLLING FUSION*

Received for publication, April 16, 2002, and in revised form, July 31, 2002
Published, JBC Papers in Press, August 6, 2002, DOI 10.1074/jbc.M203704200

Oliver M. Schlüter‡§¶, Mikhail Khvotchev¶‖, Reinhard Jahn§, and Thomas C. Südhof‖

From the ‡Max-Planck-Institut für experimentelle Medizin and §Max-Planck-Institut für biophysikalische Chemie, 37075 Göttingen, Germany and the ‖Department of Molecular Genetics, Center for Basic Neuroscience, and Howard Hughes Medical Institute, University of Texas Southwestern Medical Center, Dallas, Texas 75390-9111

Rab3A, Rab3B, Rab3C, and Rab3D constitute a family of GTP-binding proteins that are implicated in regulated exocytosis. Various localizations and distinct functions have been proposed for different and occasionally even for the same Rab3 protein. This is exemplified by studies demonstrating that deletion of Rab3A in knock-out mice results in dysregulation of the final stages of exocytosis, whereas overexpression of Rab3A in neuroendocrine cells causes nearly complete inhibition of Ca^{2+}-triggered exocytosis. We have now examined the properties of all Rab3 proteins in the same assays, with the long-term goal of identifying a common conceptual framework for their functions. Using quantitative immunoblotting, we found that all four Rab3 proteins were expressed in brain and endocrine tissues, although at widely different levels. Rab3A, Rab3B, and Rab3C co-localized to synaptic and secretory vesicles consistent with potential redundancy, whereas Rab3D was expressed at high levels only in the endocrine pituitary (where it was more abundant than Rab3A, Rab3B, and Rab3C combined), in exocrine glands, and in adipose tissue. In transfected PC12 cells, all four Rab3 proteins strongly inhibited Ca^{2+}-triggered exocytosis. Except for a mutation that fixes Rab3 into a permanently GDP-bound state, all Rab3 mutations tested had no effect on this inhibition, including a mutation in the calmodulin-binding site that was described as inactivating (Coppola, T., Perret-Menoud, V., Lüthi, S., Farnsworth, C. C., Glomset, J. A., and Regazzi, R. (1999) *EMBO J.* 18, 5885–5891). Unexpectedly, overexpression of wild type Rab3A and permanently GTP-bound mutant Rab3A in PC12 cells caused a loss of secretory vesicles and an increase in constitutive, Ca^{2+}-independent exocytosis that correlated with the inhibition of regulated Ca^{2+}-triggered exocytosis. Our data indicate that overexpression of Rab3 in PC12 cells impairs the normal control of the final step in exocytosis, thereby converting the regulated secretory pathway into a constitutive pathway. These results offer an hypothesis that reconciles Rab3 transfection and knock-out studies by suggesting that Rab3 functions as a gatekeeper of a late stage in exocytosis.

Rab3 proteins form a family of related GTP-binding proteins called Rab3A, Rab3B, Rab3C, and Rab3D that function in regulated exocytosis. Rab3A is an abundant synaptic vesicle protein (1) and the most abundant Rab protein in the brain (2). Rab3C has also been localized to synaptic vesicles, and both Rab3A and Rab3C coordinately dissociate from synaptic vesicles during exocytosis (3, 4). Rab3D is expressed primarily outside the brain in exocrine glands and in mast cells where it is enriched on secretory vesicles (5–7), but conflicting data have been reported about the localization of Rab3B (8–10).

Few proteins have been endowed with as many contradictory attributes as Rab3. For example, co-expression of multiple Rab3s was observed in several cell types, but some studies describe a differential localization of different Rab3s in the same cell (10–12), whereas other studies find a similar localization (4). In some reports, transfection experiments have revealed that Rab3 proteins have distinct, isoform-specific functions (13), but in other studies they were associated with similar functions (14, 15). Furthermore, even for the same Rab3 protein, different approaches have suggested distinct, non-overlapping functions. For example, deletion of Rab3A in knock-out mice leads to a relatively mild phenotype that includes altered short-term synaptic plasticity and the absence of a presynaptic form of long-term potentiation (16, 17). Transfection of Rab3A into PC12 cells and chromaffin cells, by contrast, causes a dramatic phenotype resulting in an almost complete inhibition of exocytosis (14, 18, 19). Moreover, the knock-out data indicate a role for Rab3A unrelated to vesicle docking (16), but microscopy studies of PC12 cells overexpressing Rab3A suggest a function in vesicle docking (20).

Based on these data and many others in the literature, it has been difficult to formulate a coherent hypothesis about the localization and functions of Rab3 proteins. One potential problem is that many studies have examined only a subset of Rab3 proteins, making it impossible to compare results from different studies. Another potential problem is that all assays of Rab3 function, be it knock-out mice or transfected cells, have distinct limitations and are inherently indirect. For example, the relatively mild phenotype in the Rab3A knock-out could be a misleading consequence of redundancy among Rab3 isoforms, whereas the inhibition of exocytosis by transfected Rab3A in PC12 cells could be because of defective biogenesis of vesicles and may be unrelated to exocytosis as such. To address these problems, at least partially, we have now directly compared the localization of all four Rab3 proteins using specific, standardized antibodies and quantitation of the protein levels. In addition, we have explored the mechanism by which Rab3 proteins inhibit exocytosis in transfected PC12 cells. We find that although the four Rab3 proteins are differentially distributed in vertebrates, all Rab3s appear to be localized on secretory vesicles. This observation suggests similar functions for and po-

* The costs of publication of this article were defrayed in part by the payment of page charges. This article must therefore be hereby marked "*advertisement*" in accordance with 18 U.S.C. Section 1734 solely to indicate this fact.

The nucleotide sequence(s) reported in this paper has been submitted to the GenBank™/EBI Data Bank with accession number(s) AF312036 and AF312037.

¶ These authors contributed equally to the present study.

** To whom correspondence should be addressed: Center for Basic Neuroscience and Howard Hughes Medical Institute, University of Texas Southwestern Medical Center, NA4.118, 6000 Harry Hines Blvd., Dallas, TX 75390-9111. E-mail: Thomas.Sudhof@UTSouthwestern.edu.

tential redundancy among Rab3 proteins, as confirmed by the finding that all four Rab3s strongly inhibited exocytosis in transfected PC12 cells. However, when we examined the mechanism of this inhibition using a series of mutants of Rab3A, the best studied Rab3 protein, we found that Rab3A overexpression did not directly inhibit exocytosis. Instead, Rab3A overexpression activated Ca^{2+}-independent constitutive exocytosis, indicating that Rab3A is essential for a normal regulation of the final step of exocytosis. These findings agree well with studies of the Rab3A knock-out mice, which also suggested a selective role of Rab3A in the terminal stages of exocytosis.

EXPERIMENTAL PROCEDURES

Materials—Enzymes for DNA manipulations were from Roche Molecular Biochemicals or New England Biolabs (Beverly, MA), fluorescence-labeled secondary antibodies from Jackson ImmunoResearch Laboratories (West Grove, PA), horseradish peroxidase-labeled secondary antibodies from BioRad, ^{125}I-labeled secondary anti-rabbit antibody from Amersham Biosciences, Eupergit C1Z methacrylate microbeads from Röhm Pharma (Darmstadt, Germany), Ni-NTA-agarose from Qiagen (Hilden, Germany), Triton X-114 from Pierce, and nitrocellulose membranes (Protran) from Schleicher & Schuell (Dassel, Germany). All other reagents were purchased from Sigma.

Antibodies—Rab3 antisera were raised as described (21) in rabbits against mouse full-length Rab3B containing a C-terminal hexahistidine tag (U953 and U954), full-length Rab3D with an N-terminal hexahistidine tag (SA5838 and SA5839), or keyhole limpet hemocyanin-coupled peptides with the following amino acid sequences: CASATDSRYGQKES (583; residues 2–14 of mouse Rab3A); CNGKPALGDTP (αR3D#2, SA5834; residues 201–211 of mouse Rab3D); and ASEPPASPRDAAC (αR3D#3, SA5837; residues 2–13 of mouse Rab3D). The monoclonal antibodies to Rab3 (Cl42.1 and Cl42.2 (22)), Rab5 (Cl621.3 (23)), synaptobrevin 2 (Cl69.1 (24)), NR1 (Cl54.1 (25)), and synaptophysin I (Cl7.2 (26)) and the rabbit polyclonal antibodies to endobrevin (27), Rab3C (R9, P180, and P181 (4,17)), rabphilin (I734 (28)), and synaptophysin II (αp37 (29)) were described previously. Polyclonal antibodies to Sec61α and LIMP-II were gifts of Dr. E. Hartmann and Dr. S. Höning, respectively (both at the University of Göttingen, Germany). Commercial sources were used for the following antibodies: anti-hexahistidine (mouse anti-peptide RGSHHHH, Qiagen), RIM 1 (Transduction Laboratories, Lexington, KY), and synaptophysin I (580, Synaptic Systems, Göttingen, Germany).

Immunoblotting—Samples were diluted with sample buffer (3% SDS, 50 mM Tris/HCl, 10% glycerol, 50 mM dithiothreitol, 0.1% bromphenol blue), heated at 50 °C for 10 min, separated by discontinuous SDS-PAGE (30), transferred onto nitrocellulose membranes (31), and probed by immunoblotting using horseradish peroxidase-labeled secondary antibodies and enhanced chemiluminescence detection (ECL; Amersham Biosciences) or ^{125}I-labeled secondary antibodies and quantification with a Fujix BAS-5000 (Ray Test, Straubenhardt, Germany) detector (32). Rab3A, Rab3B, Rab3C, and Rab3D were distinguished from each other based on isoform-specific antibodies (see Fig. 1) and migration size. For analysis of tissue samples, hydrophobic proteins of rat tissue homogenates were enriched by phase partitioning in Triton X-114 (33). Tissues were homogenized in 10 volumes of homogenization buffer (0.32 M sucrose, 5 mM HEPES-NaOH, pH 7.4, 0.1 mM EDTA, 200 μM phenylmethylsulfonyl fluoride) with an ultra-turrax (lung, skeletal muscle, heart muscle) or a glass-Teflon potter (all other tissues). Equal protein amounts of total homogenates (lung and skeletal and heart muscles) or postnuclear supernatants (all other tissues) were extracted as described (32, 33), and aliquots of the detergent phase corresponding to 75 μg of the starting homogenate were analyzed by immunoblotting. All blots were standardized by including known amounts of heterologously expressed His-tagged Rab3 proteins. Peak areas were background-subtracted and normalized to signals of recombinant Rab3 to allow comparison between various Rab isoforms and between different blots, with Rab3A concentrations in the brain cortex as the reference point (100%). For LIMP-II and endobrevin, the signal of the tissue with the highest amount was taken as the reference point.

Immunocytochemistry—Anesthetized adult mice were perfused transcardially with PBS followed by 4% paraformaldehyde in PBS. Brains were cryoprotected and cut into 20-μm frontal sections on a cryomicrotome (CM1325, Leica, Bensheim, Germany) as described (34). Slices were stored in antifreeze (25 mM sodium phosphate buffer, pH 7.3, 30% ethylene glycol, 20% glycerol) at −20 °C. Immunostaining was performed as described (32, 34). Sections were mounted on gelatin-coated microscopic slides with *N*-propylgallate (1,5% in 60% glycerol in PBS) and viewed in an epifluorescence (Axiophot, Zeiss, Göttingen, Germany) or confocal microscope (MRC-1024, BioRad).

Expression Vectors—For generation of N-terminally hexahistidine-tagged expression constructs, mouse Rab3A (primers 1236, CGGGATCCGCTTCCGCCACAGACTCTCGC, and 1209, TCAGCAGGCACAATCCTGATGAGG), Rab3B (primers 931, CATATGGCTTCAGTGACTGATGGTAAGACTGG and 932,GAATTCTGCTGCAGCAGAGGTGGGG-),and Rab 3C (primers 1238, GGATCCGCCTCTGCACAAGATGCCAGG, and 1213, TTAGCAGCCACAGTTGGGCTGTGG) were cloned by PCR from mouse brain cDNA as template. Mouse Rab3D (primers 1239, CGGGATCCGCATCCGCTAGTGAGCCCCC, and 1212, CTAACAGCTGCAGCTGCTCGGCTG) cDNA was amplified from a plasmid (gift of Dr. H. Lodish, Cambridge, MA). The PCR products were cloned into pBluescript II containing a translation initiation sequence and the N-terminal hexahistidine tag (introduced by primers 1234, CTAGAAAGCTTTCCACCATGAGAGGATCGCAT CACCATCACCATCACG, and 1235, (GATCCGTGATGGTGATGGTGATGCGATCCTCTCATGGTGGAAAGCTTT), and the complete inserts were transferred into the eukaryotic expression vector pcDNA3. A series of Rab3 expression vectors was constructed for cotransfection studies in PC12 cells (Table I). Wild type constructs lacking the N-terminal histidine tag were amplified with the primers 2029 (CGGGATCCACCATGGCTTCCGCCACAGACTCTCGCTAT) and 2037 (GGAATTCTC AGCAGGCACAATCCTGATGAGG) for Rab3A, 2038 (CGGGATCCACCATGGCTTCAGTGACTGAT GGTAAGACTGG) and 2039 (GGAATTCCTAGCAAGAGCAGTTCTGCTGGAG) for Rab3B, 2040 (CGGGATCCACCA TGAGACACGAGGCGCCCATGCAGATGGCCTCTGCACAAGATGCCAGGTTTG) and 2043 (GGAATTCTTAGCA GCCACAGTTGGGCTGTGG) for Rab3C, and 2044 (CGGGATCCACCATGGCATCCGCTAGTGAGCCCCCT) and 2047 (GGAATTCCTAACAGCTGCAGCTGCTCGGCTG) for Rab3D. Mutations were introduced by PCR with the following primers: 2029, 2031 (GGTGCGGTACCGCTCTAGACCTGCTGTGTCCC), 2030 (GGGACACAGCAGGTCTAGAG CGGTACCGCACC), and 2037 for Rab3A Q81L; 2029, 2438 (GACCTTGGAGTCTATGCCAACGGTGCTG), 2437 (CAGCACCGTTGGCATAGACTCCAAGGTC), and 2037 for Rab3A F59S; 2029, 2461 (CCTGGGCATTGTC CGTCGAGTAAGTT), 2460 (AACTTACTCGACGGACAATGCCCAGG), and2037 for Rab3A W125T; 2340 (TGATCATTGGGAACAGCAGCGTGGGCAAAAACTCGTT) and 2037 for a fragment replacing the *Bcl*I and *Eco*RI wild type sequence and generating Rab3A T36N; 2029 and 2361 (AGATCTGCAGCTTGATCGTCTTGTCGTTGAGGTAGATG) for a fragment replacing the *Bam*HI and *Bgl*II wild type sequence and generating Rab3A R66L R70T; and 2038 and 2339 (CTGCAGCTTCACAGTCTTCTCATGGAGGTAGACT) for a fragment replacing the *Bam*HI and *Pst*I wild type sequence and generating Rab3B R66L R70T. Bacterial expression vectors for antigens for immunization were generated as follows. Rab3B was amplified with the primers 931 (CATATGGCTTCAGTGACTGATGGTAAGACTGG) and 932 (GAATTCTGCTGCAGCAGAGGTGGGG) and subcloned into the vector pHO2c (modified pET2, Novagen, Madison, WI), resulting in a C-terminal hexahistidine tag for affinity purification over Ni-NTA-agarose. Rab3D was amplified with primers with the sequence CGCATATGGCATCCGCTAGTG and GCGGATCCTAACAGCTGCAGC and subcloned into pET15b (Novagen), resulting in an N-terminal hexahistidine tag for affinity purification. Bacterial expression was performed in *Escherichia coli* strain BL21(DE3). All constructs were verified by sequencing. Mouse Rab3B and Rab3C sequences were submitted to GenBank™ (accession numbers AF312036 and AF312037).

Measurements of hGH[1] Secretion from Intact PC12 Cells—PC12 cells (obtained from the ATCC) were maintained in RPMI 1640 medium containing 10% heat-inactivated horse serum, 5% fetal bovine serum, and penicillin and streptomycin (50 u/ml each) at 37 °C in a 5% CO_2 humidified atmosphere. PC12 cells were split from a confluent flask and seeded after vigorous trituration onto 6-well plates (35-mm diameter) to achieve 50–60% confluence on the day of transfection. Typically, 1 μg of phGH-CMV5 and 1 μg of test plasmid DNA/well were co-transfected using Fugene 6 transfection reagent (Roche Molecular Biochemicals) at a ratio of 1:3 (μg: μl) according to the manufacturer's specifications. 2–3 days after transfection, PC12 cells were collected and replated onto collagen-coated 12-well plates (22-mm diameter) at a ratio of four 22-mm wells/each transfected 35-mm well. The next day, cells were briefly rinsed with Krebs bicarbonate buffer (KBB; 118 mM NaCl, 25

[1] The abbreviations used are: hGH, human growth hormone; KBB, Krebs bicarbonate buffer; PBS, phosphate-buffered saline; SNARE, soluble NSF attachment protein receptors.

mM $NaHCO_3$, 3.5 mM KCl, 1.25 mM $CaCl_2$, 1.2 mM $MgSO_4$, 1.2 mM KH_2PO_4, 11.5 mM glucose, 5 mM HEPES-NaOH, pH 7.5), and incubated for 15 min at 37 °C in 5% CO_2 atmosphere with KBB (for basal secretion) or stimulating media (high potassium KBB: 56 mM KCl and 59.5 mM NaCl; or 0.5 nM α-latrotoxin in KBB). Assay media were cleared by centrifugation at 1000 × *g* for 4–5 min, and EDTA was added to 4–5 mM. Corresponding PC12 cells were lysed in PBS containing 1 mM EDTA and 0.5 mM phenylmethylsulfonyl fluoride by three cycles of rapid freezing and thawing. Resulting cell extracts were cleared by high-speed centrifugation. The amounts of hGH secreted into the medium and remaining in the cell extracts were quantified by radioimmunoassay (Nichols Institute Diagnostics).

Measurements of Secretion from Permeabilized PC12 Cells—Cells were transfected as described above. One 6-well plate was used per each construct. 3–4 days after transfection, cells were collected and divided into two groups. One part, equivalent to the amount of PC12 cells in one 35-mm well, was re-plated onto four collagen-coated 22-mm wells and processed for the standard secretion assays from intact PC12 cells. The remainder of the transfected cells was used in cracked PC12 cell secretion assays modified from Klenchin *et al.* (35). Cells were washed with KBB followed by a second washing with ice-cold KGlu buffer (120 mM potassium glutamate, 20 mM potassium acetate, 2 mM EGTA, 20 mM HEPES-NaOH, pH 7.2). Cells were resuspended in 6 ml of KGlu buffer and permeabilized by freezing at −80 °C overnight followed by slow thawing at room temperature. EGTA was added to 10 mM, and cells were left on ice for 1–2 h to allow efficient extraction of cytosolic proteins. Resulting cell ghosts were washed 2–3 times with KGlu buffer containing 1 mg/ml bovine serum albumin. PC12 cell ghosts prepared from one 6-well plate were used in 20–32 assay reactions. Each reaction mixture contained washed PC12 cell ghosts, 2 mM Mg-ATP, 10% rat brain cytosol (6–10 mg/ml total protein), and varying concentrations of calcium in the total reaction volume of 200 μl of KGlu buffer. Free Ca^{2+} concentrations in the EGTA-Ca^{2+} buffer were calculated using EqCal software (Biosoft). Reactions were incubated at 30 °C for 20 min, chilled on ice, and centrifuged at 3,000 *g* for 10 min. To determine total cellular hGH levels, pelleted PC12 ghosts were lysed in PBS containing 1 mM EDTA and 0.5 mM phenylmethylsulfonyl fluoride by three cycles of rapid freezing and thawing. Resulting ghost extracts were cleared by high-speed centrifugation. The amounts of hGH secreted into the medium and remaining in the PC12 ghost extracts were quantified by radioimmunoassay (Nichols Institute Diagnostics).

Subcellular Fractionations—Isolation of small synaptic vesicles was done as described previously (36). For immunoisolation of organelles, monoclonal antibodies Cl69.1 (anti-synaptobrevin 2), Cl42.2 (anti-Rab3A), and Cl621.3 (anti-Rab5) were coupled covalently to Eupergit C1Z methacrylate microbeads, and isolations from rat brain homogenates were performed as described previously (37, 38). To study the effects of overexpression of Rab3A on subcellular localization of hGH, PC12 were co-transfected with the hGH expression vector and either the empty control vector or the Rab3 expression vector as described above. Three days after transfections, PC12 cells were labeled overnight with [^{3}H]norepinephrine (Amersham Biosciences, 6 μCi, 30–50 Ci/mmol/6-well plate) in the presence of 0.5 mM ascorbic acid. The next day, cells were washed with KBB, resuspended in 0.25 ml of ice-cold water, and incubated for 5 min on ice. Cell suspension was diluted with an equal volume of 2× TNE buffer (1× = 150 mM NaCl, 2 mM EGTA, 20 mM Tris-HCl, pH 7.5), and passed 10 times through a 28.5-gauge needle. Cell homogenate was centrifuged twice at 800 × *g* for 10 min to obtain postnuclear supernatant. 0.4 ml of postnuclear supernatant was loaded onto 10 ml of discontinuous sucrose gradients made of 2-ml steps of 0.25, 0.5, 1, 1.5, and 2 M sucrose in TNE buffer and centrifuged at 35,000 rpm for 2.5 h (SW41 rotor ~200,000 × *g*). Fractions of 0.5–0.6 ml were collected from the top of the gradients. The amounts of norepinephrine in the fractions were determined directly by liquid scintillation counting. To measure hGH, fractions were diluted with PBS, subjected to three cycles of rapid freezing and thawing, and analyzed by radioimmunoassay. For analysis of protein markers, fractions were diluted 10 times with TNE buffer and centrifuged overnight at 200,000 × *g*. Membranes were resuspended in SDS-PAGE loading buffer and analyzed by immunoblotting.

Quantitation of Extracellular hGH—PC12 cell transfections were performed as described for the secretion assays. Aliquots of the extracellular media (50 μl) were collected on days 2, 3, and 4 after transfection, diluted 10 times with PBS containing 5 mM EDTA, and assayed for hGH. On day 4 after transfection, the PC12 cells were collected, washed with PBS, and lysed by three cycles of freezing and thawing to determine the intracellular hGH. The amount of hGH secreted into the culture media on days 2, 3, and 4 was normalized in comparison with the amount of hGH remaining in PC12 cells at the day 4.

Miscellaneous—Protein concentrations were determined using the BCA method (Pierce) according to the manufacturer's specifications. RNA blotting experiments were performed with isoform-specific probes and commercial RNA blots (obtained from Clontech Inc.).

RESULTS

Generation of Isoform-specific Rab3 Antibodies—Although prior studies have examined the tissue distributions of Rab3 proteins (*e.g.* see Ref. 39), no study has compared all four Rab3 proteins, and no measurements of the relative levels of different Rab3s have been attempted. One of the four Rab3 proteins, Rab3B, has not even been studied yet at the protein level, presumably because of a lack of specific antibodies. Therefore our first goal was to generate specific antibodies to all four Rab3 proteins, and to measure their sensitivity and specificity. We chose to study Rab3 proteins with antibodies instead of simply measuring the Rab3 mRNAs because it is difficult to quantify mRNA levels for comparisons between different proteins and because mRNA levels often do not correlate with protein levels; this proved to be particularly true for Rab3 proteins (see below).

We characterized a total of nine antibodies to the four Rab3 proteins, using either newly generated (583, U953, U954, αR3D#2, αR3D#3, SA5838, and SA5839) or previously characterized antibodies (Cl42.1 and 42.2; P180 and P181; Refs. 17 and 22). The antibodies were examined with recombinant Rab3A, 3B, 3C, and 3D proteins that were produced as fusion proteins with an N-terminal histidine tag in transfected 293 cells. The Rab3 proteins were synthesized in the transfected cells at different levels. To obtain cells with the same overall protein concentrations and the same amounts of the respective recombinant Rab3 proteins, we adjusted extracts from transfected 293 cells with extracts from untransfected 293 cells until equivalent signals were obtained with an antibody to the hexahistidine tag attached to all recombinant Rab3 proteins. Cell extracts containing nearly identical amounts of Rab3A, Rab3B, Rab3C, or Rab3D were then analyzed by immunoblotting with the various antibodies.

Fig. 1 shows that most of the antibodies we tested were either completely specific or nearly specific for the Rab3 protein against which they are raised, providing us with the tools required for examining the level and localization of the respective Rab3 proteins in tissues. Only two antibodies reacted with all four Rab3 proteins: the previously described monoclonal antibody Cl42.1 (22, 40), which, however, only weakly recognized Rab3D, and the newly generated antibody SA5839 (against full-length mouse Rab3D), which reacted preferentially with Rab3D (Fig. 1). Rab3 proteins display distinct migration patterns that can be used as an identifying mark in addition to the specificity of the antibodies. Although Rab3C, due to the presence of eight additional N-terminal amino acids, has the highest calculated molecular weight, Rab3D exhibited the slowest electrophoretic mobility, followed by Rab3C, 3A, and 3B (Fig. 1). It should be noted that in transiently transfected 293 cells, the post-translational geranylgeranylation of Rab3 proteins is incomplete, presumably because the overexpressed proteins overwhelm the geranylgeranylation capacity of the cells (41). As a result, an immature lower band and a mature upper band are observed for Rab3 proteins in transfected 293 cells but not in rat tissue samples (Fig. 1, data not shown).

Tissue Distribution of Rab3 Proteins—To quantify the levels of Rab3A, Rab3B, Rab3C, and Rab3D in different organs, we first extracted fractions from 18 rat tissues with Triton X-114 to enrich for hydrophobic proteins (33). This was done to increase the sensitivity of detection of Rab3 proteins. Rab3 proteins are hydrophobic, because of their C-terminal geranylgera-

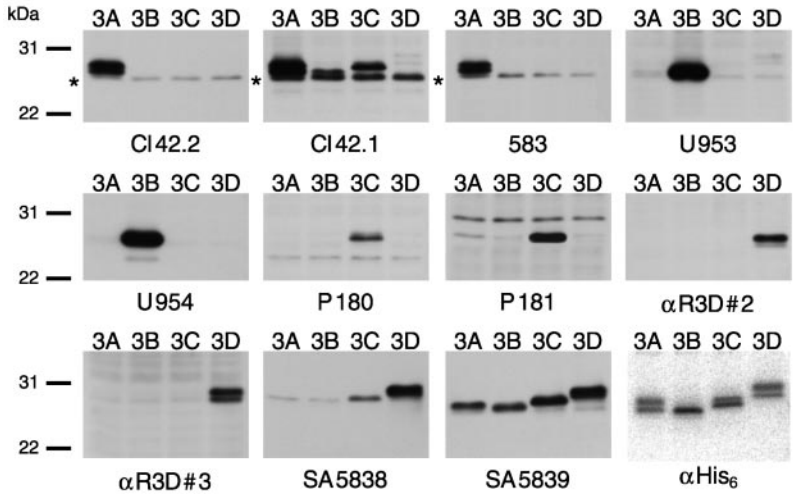

FIG. 1. **Standardization of antibodies to Rab3A, Rab3B, Rab3C, and Rab3D.** Murine Rab3A, Rab3B, Rab3C, and Rab3D were expressed in 293 cells by transient transfection as fusion proteins with an N-terminal six-histidine (hexahistidine) tag. Five days after transfection, postnuclear supernatants were prepared and analyzed by SDS-PAGE and immunoblotting (20 μg protein/lane) using the indicated two monoclonal antibodies (*Cl42.2* and *Cl42.1*) and nine polyclonal antibodies (*583*, *U953*, *U954*, *P180*, *P181*, *αR3D#2*, *αR3D#3*, *SA5838*, and *SA5839*). In addition, samples were blotted with an antibody against the hexahistidine tag (αHis_6) because the hexahistidine tag is present on all Rab3s and can thus be used to standardize the amounts of Rab3 proteins loaded. Samples were adjusted so that each contained the same amount of Rab3 protein as measured with the αHis_6 antibody by diluting the extracts from transfected cells with extracts of untransfected cells. Signals were visualized using horseradish peroxidase-coupled secondary antibodies and ECL, as shown here, or ^{125}I-labeled secondary antibodies and phosphorimaging detection for quantitation (not shown). An *asterisk* indicates cross-reactivity of the antibodies with a human protein in 293 cells.

nyl modification, and are co-purified with membrane proteins by Triton X-114 extraction (41, 42). We then measured the amount of each Rab3 protein relative to a standard amount of heterologously expressed Rab3 analyzed on the same blot; immunoblotting signals were quantified using ^{125}I-labeled secondary antibodies and detected by phosphorimaging. As positive controls, the broadly distributed lysosomal protein LIMP-II and the endosomal protein endobrevin were examined on the same blots. Because the antibody signals were normalized via the common histidine tag present on all recombinant Rab3 standards, it was possible to express the total amount of each Rab3 protein in relation to Rab3A, using the amount of Rab3A in brain cortex as the reference point (Fig. 2).

As expected, protein quantification showed that Rab3A was the most abundant Rab3 isoform in brain and was largely co-distributed with Rab3C in the brain and the pituitary gland (4). Rab3B, however, was also detected in all brain areas and was most abundant in the pituitary (Fig. 2). These findings were confirmed by immunoblotting analyses of different brain areas, which revealed that Rab3A is uniformly present throughout the brain, whereas Rab3B was expressed at high levels only in the olfactory bulb and the pituitary, and Rab3C was synthesized at variable levels in all brain areas (Fig. 3*A*). The overall distribution of Rab3D was strikingly different from that of Rab3A, Rab3B, and Rab3C, which are largely co-expressed in neuronal and endocrine tissue (Fig. 2). Rab3D was also detected in the brain, albeit at very low levels, but was observed at unexpectedly high concentrations in the pituitary, where it constituted the most abundant Rab3 protein (Figs. 2 and 3*B* and data not shown). Dissection of the pituitary into adeno- and neurohypophysis revealed that Rab3 proteins are differentially distributed, with Rab3A and 3C expressed primarily in the neurohypophysis and Rab3B and Rab3D in the adenohypophysis (Fig. 3*B*). As described previously (5–7), the highest amounts of Rab3D were measured in the lachrymal, parotid, and submandibular glands and the pancreas. The absolute levels of Rab3D in lachrymal and parotid glands were twice as high as those of Rab3A in brain (Fig. 2). Rab3D was also broadly distributed outside of the pituitary and exocrine glands, for example in lymph nodes and adipose tissues as described previously (43). In many tissues, however, we did not detect significant amounts of any Rab3 protein, most notably in the lung, liver, kidney, testis, and spleen. The control membrane proteins LIMP-II and endobrevin were quite abundant in all of these tissues that together make up the bulk of the body mass outside of the brain. The absence of Rab3A protein in the testis was surprising in view of extensive previous data describing Rab3A as an important mediator of acrosomal fusion in sperm (15, 44, 45) but agrees well with the fact that Rab3A knock-out males are fertile (2).

In addition to the immunoblotting analyses, we performed RNA blotting experiments to test whether Rab3 mRNA and protein levels correlate. As expected, the highest mRNA signals for Rab3A, Rab3B, and Rab3C were observed in the brain (data not shown). Unexpectedly, however, we found significant levels of Rab3A mRNA in the lung and testis even though no protein was detectable in these tissues. Similarly, we observed relatively high mRNA levels for Rab3D in the lung in the absence of Rab3D protein (data not shown). These results show that the mRNA levels of a Rab3 protein are not necessarily indicative of protein expression in a tissue, although it is unclear whether there is translational regulation that depresses production of Rab3 proteins in these tissues or whether the synthesized Rab3 proteins are unstable and degraded in these tissues.

Co-localization of Rab3A, 3B, and 3C on Synaptic Vesicles—To determine whether all three Rab3 proteins that are abundant in the brain, Rab3A, Rab3B, and Rab3C, are present on synaptic vesicles, we performed subcellular fractionations (Fig. 4 and data not shown) and immunocytochemistry (Fig. 5). We purified synaptic vesicles by differential centrifugation followed by controlled pore-glass chromatography, currently the most rigorous purification method of synaptic vesicles (36). Fig. 4 shows that Rab3B co-purified with Rab3A and synaptophysin, a well established synaptic vesicle protein (26), suggesting that Rab3B is also a synaptic vesicle protein. To test this conclusion by an independent approach, we performed organelle immunoprecipitation from the brain with antibodies to synaptobrevin 2 (a SNARE protein of synaptic vesicles), Rab3A, and Rab5 (a Rab protein that is equally present on synaptic vesicles and several other intracellular membranes

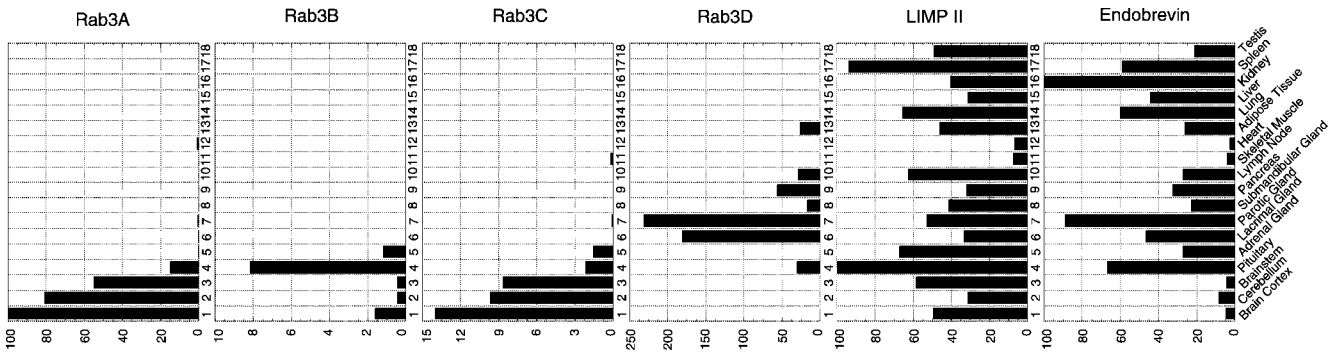

FIG. 2. **Quantitation of the relative expression of Rab3A, Rab3B, Rab3C, and Rab3D in rat tissues.** Homogenates of the indicated rat tissues were extracted with Triton X-114 to enrich for Rab3 proteins that carry a C-terminal geranylgeranyl modification, which renders them hydrophobic. Equivalent amounts of proteins (corresponding to 75 μg of starting material) were analyzed by SDS-PAGE and immunoblotting with antibodies to Rab3A (Cl42.2), Rab3B (U954), Rab3C (P180), and Rab3D (aR3D#2) (see Fig. 1). Signals were quantified using ^{125}I-labeled secondary antibodies on a Fujix BAS-5000. Equal amounts of heterologously expressed Rab3 proteins were analyzed on each blot, and signal intensities were standardized. All values are normalized for the amount of Rab3A in the brain cortex (100%). As a positive control, all samples were examined with antibodies to the ubiquitous intracellular proteins LIMP-II and endobrevin (*bottom two panels*). The data for the control proteins were normalized to the levels in tissues that contain the highest amounts of LIMP-II and endobrevin (pituitary and kidney, correspondingly).

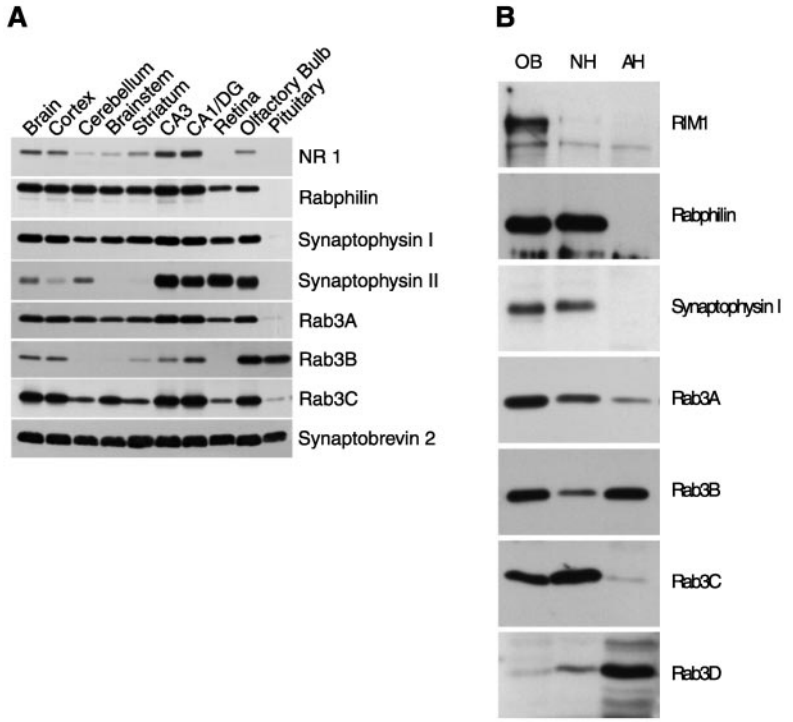

FIG. 3. **Distribution of Rab3A, Rab3B, Rab3C, and Rab3D in brain and pituitary.** *A*, proteins in the postnuclear supernatant from the mouse brain regions shown were analyzed by immunoblotting with antibodies to the indicated proteins (*NR 1*, NMDA-receptor subunit 1). Note the relative enrichment of Rab3B in the pituitary. *B*, immunoblot analysis of proteins in postnuclear supernatants from rat olfactory bulb (*OB*), neurohypophysis (*NH*), and adenohypophysis (*AH*) with antibodies to the indicated proteins. In *A* and *B*, ~30 μg of protein/lane were analyzed, and signals were visualized by ECL.

(23)). Immunoprecipitated organelles (see "Experimental Procedures" and Ref. 37) were highly enriched in synaptophysin as a synaptic vesicle marker and contained abundant amounts of Rab3A, Rab3B, and Rab3C (data not shown). This result confirms that Rab3A, Rab3B, and Rab3C are all present on synaptic vesicles, suggesting a greater range of potential redundancy among Rab3 proteins than previously anticipated. To examine how much the localization of Rab3B overlaps with that of Rab3A, we studied the distribution of Rab3A and 3B in olfactory bulb by immunocytochemistry (Fig. 5). Olfactory bulb was chosen for these experiments because it contains relatively high levels of Rab3B (see *lane 1*, Fig. 3*B*). Immunofluorescence double labeling of cryostat sections revealed that Rab3A was widely distributed in the olfactory bulb, whereas Rab3B was present in a more restricted pattern. All Rab3B-positive structures were also labeled by Rab3A antibodies, although many Rab3A-positive structures did not contain Rab3B (see *right panels* in Fig. 5). Because Rab3A was previously shown to be synaptic (1, 22), this result indicates that Rab3B is present in synapses and that all synapses containing Rab3B also contain Rab3A, although Rab3A appears to be present in a large number of synapses without Rab3B.

Rab3 Proteins Inhibit Ca^{2+}-triggered Exocytosis in PC12 Cells Independently of Interactions with Potential Target Molecules—The co-distribution of Rab3A, Rab3B, and Rab3C on synaptic vesicles in the brain, the corresponding localization of Rab3D on secretory vesicles in exocrine glands, and the overall sequence homology between these proteins suggest similar functions in regulated secretion. Consistent with this hypothesis and with previous results (14, 15), transfection of all four Rab3s severely inhibited Ca^{2+}-triggered exocytosis (Fig. 6). This was measured by testing the effect of a co-transfected Rab3 protein on the exocytosis of transfected human growth hormone (hGH) in PC12 cells stimulated by K^+-depolarization or with α-latrotoxin. As a negative control, an empty expression vector was co-transfected with hGH. The Rab3-dependent inhibition of Ca^{2+}-triggered exocytosis was not caused by impairment of voltage-gated Ca^{2+}-channels because the inhibition

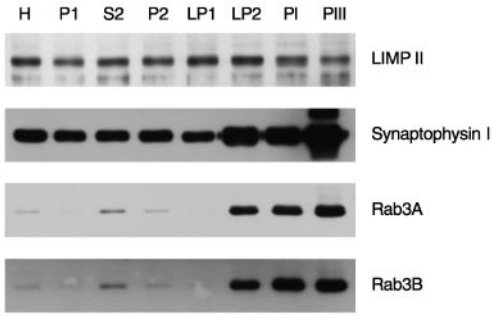

FIG. 4. **Localization of Rab3A and 3B to synaptic vesicles.** Immunoblot analysis of fractions obtained during the purification of synaptic vesicles by differential centrifugation and controlled pore-glass chromatography. Equivalent amounts of proteins were analyzed by immunoblotting using antibodies to the lysosomal membrane protein LIMP-II as a negative control and to the synaptic vesicle protein synaptophysin 1 as a positive control in addition to antibodies to Rab3A and Rab3B. *H*, homogenate; *P1*, crude nuclear pellet; *S2*, 10,000 × *g* supernatant; *P2*, crude synaptosomes (10,000 × *g* pellet); *LP1*, 25,000 × *g* pellet obtained after synaptosomal lysis; *LP2*, crude synaptic vesicles (100,000 × *g* pellet); *PI* and *PIII*, large membrane and purified synaptic vesicle fractions, respectively, as separated by controlled-pore glass bead chromatography (for details, see Refs. 36 and 52).

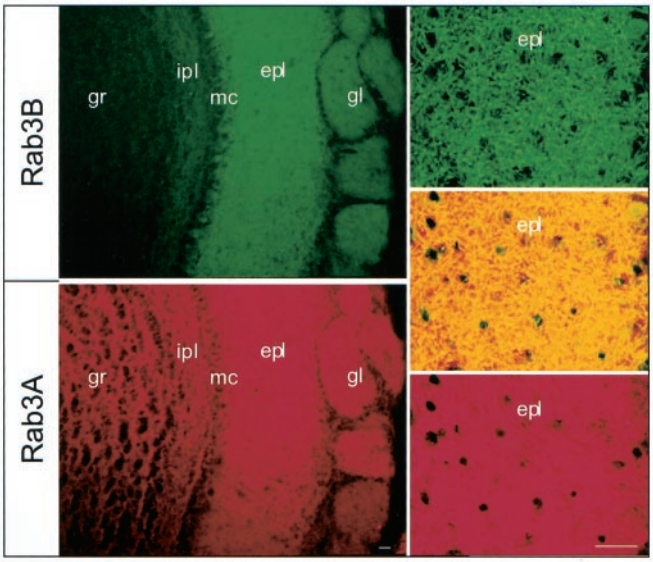

FIG. 5. **Immunofluoresence localization of Rab3A and Rab3B in the olfactory bulb.** A cryosection of mouse olfactory bulb (20-μm thickness) was double-labeled with antibodies to Rab3A (*red* signals) and Rab3B (*green* signals). Panels on the *left* show low-power overviews obtained with an epifluorescence microscope (*bar* = 30 μm), and panels on the *right* show high-power views produced with a confocal microscope (the *central panel* on *right* depicts the merged signal, with the overlap between *red* and *green* shown as *yellow*; *bar* = 20 μm). *epl*, external plexiform layer; *gl*, glomerulus; *gr*, granule cell layer; *ipl*, inner plexiform layer; *mc*, mitral cell layer.

was equally observed with K^+ depolarization (which opens Ca^{2+}-channels) and α-latrotoxin (which acts in PC12 cells by a Ca^{2+}-dependent mechanism that does not involve Ca^{2+}-channels; see Ref. 46).

The magnitude of the effect of inhibition of exocytosis by Rab3 is puzzling in view of the mildness of the Rab3A knockout phenotype (2, 16). To elucidate the mechanism of this inhibition, we first tested whether membrane attachment of Rab3A is essential for inhibition by comparing wild type Rab3A with a mutant lacking the C terminus, which is modified by geranylgeranylation (41). The C-terminally truncated Rab3A was as effective as the wild type in inhibiting Ca^{2+}-triggered exocytosis (Fig. 7*A*). This result was confirmed with Rab3A proteins that were N-terminally fused to GFP, which allowed us to visualize the transfected cells and to evaluate the locations of the transfected proteins (data not shown). In these experiments, the transfected cells appeared to express similar levels of Rab3 proteins that exhibited distinct localizations depending on their GTP-binding status. The transfected cells looked normal, without evidence of cellular pathology, indicating that the transfected proteins were not cytotoxic.

We next measured the effect of wild type and C-terminally truncated Rab3A on Ca^{2+}-triggered secretion from PC12 cells that had been cracked open by freeze-thawing after transfection of hGH and control or test plasmids. If PC12 cells are permeabilized by freeze-thawing 3 days after transfection, secretory granules containing transfected hGH remain associated with the plasma membrane in the resulting PC12 cell ghosts and can be stimulated for exocytosis by the addition of Ca^{2+} (35, 47). In the cracked PC12 cell ghosts, inhibition by wild type Rab3A was not as effective as in the whole cell assay, whereas the C-terminally truncated version was more effective (Fig. 7*B*). One possible explanation for these results is that the transfected Rab3 proteins change the Ca^{2+}-dependence of exocytosis. The more moderate inhibition by wild type Rab3A in the cracked cells could then be explained by the fact that Ca^{2+} is supplied at higher concentrations to the sites of exocytosis in the cracked cells. To address this possibility, we tested the relative inhibition of exocytosis by wild type Rab3A and by the GTP-fixed Rab3A mutant at different Ca^{2+}-concentrations (Fig. 8). In control cells, a bell-shaped Ca^{2+}-dependence of exocytosis was observed with a maximum at ~3 μM free Ca^{2+}, similar to previous results (47). In cells transfected with wild type Rab3A or the permanently GTP-bound mutant of Rab3A, exocytosis was inhibited at all Ca^{2+}-concentrations (Fig. 8). This result demonstrates that Rab3A does not simply shift the Ca^{2+}-dependence of exocytosis, and thus it acts at a step distinct from the Ca^{2+}-triggering step.

What Sequences of Rab3 Are Required for Inhibition of Exocytosis?—We tested a series of mutants of Rab3A and Rab3B that disrupt known activities of Rab3 proteins, in order to clarify a number of contradictory results in the literature, most importantly the finding that the calmodulin-binding site in Rab3A is essential for its inhibitory activity in transfected PC12 cells (48) despite the fact that calmodulin is not required for Ca^{2+}-triggered exocytosis in PC12 cells as such (49). Similar to previous findings (Ref. 14; but note Ref. 48), we observed that wild type and constitutively GTP-bound Rab3A (Q81L) were equally active in inhibiting exocytosis (Fig. 9). This finding was similarly obtained for all four Rab3 isoforms (Table I). In contrast, the constitutively GDP-bound form of Rab3A (T36N) was inactive. Furthermore, we examined a Rab3A mutant that is deficient in GTP-dependent binding of rabphilin (F59S (14)) and another point mutant of Rab3A in which a tryptophan residue that is characteristic for Rab3 proteins but absent from most other Rab proteins is replaced by a threonine (W125T). Neither of these mutations interfered with the ability of Rab3A to inhibit exocytosis (Fig. 9). Finally, we tested the mutation in the calmodulin binding site or Rab3A (R66L/R70T), which inactivated the inhibitory effect of Rab3A in previous studies (48). However, in the present experiments this mutation did not change the inhibitory effect of Rab3A (Fig. 9). To ensure that this discrepancy was not due to an incalculable peculiarity of our Rab3A clone, we inserted the same mutation into the Rab3B expression vector where it again had no effect on inhibition (Fig. 9; Table I). This result indicates that none of the currently known effectors of Rab3A is responsible for its inhibitory effect on Ca^{2+}-triggered exocytosis in PC12 cells.

Rab3A Activates Constitutive Exocytosis—The observation that Rab3A inhibits Ca^{2+}-triggered exocytosis more effectively

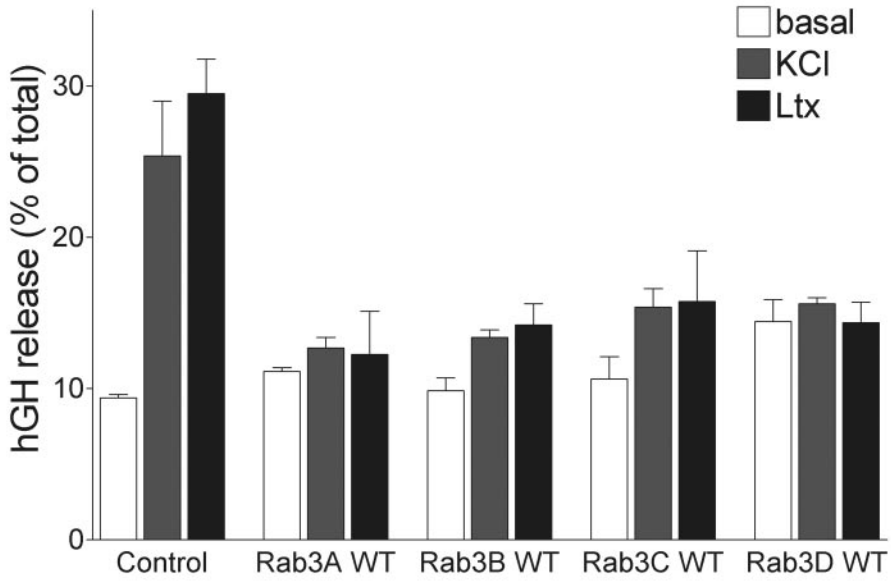

FIG. 6. **Transfected Rab3A, Rab3B, Rab3C, and Rab3D similarly inhibit PC12 cell exocytosis stimulated by KCl depolarization or by α-latrotoxin.** An expression vector encoding hGH was co-transfected into PC12 cells with an empty expression vector (control), or Rab3A, Rab3B, Rab3C, or Rab3D expression vectors. Transfected PC12 cells were then stimulated for secretion with 56 mM KCl or 0.5 nM α-latrotoxin (*Ltx*) for 15 min, and the hGH released into the medium was measured by radioimmunoassay. The data shown correspond to a single representative experiment performed in duplicate and repeated multiple times, with inhibition varying between experiments.

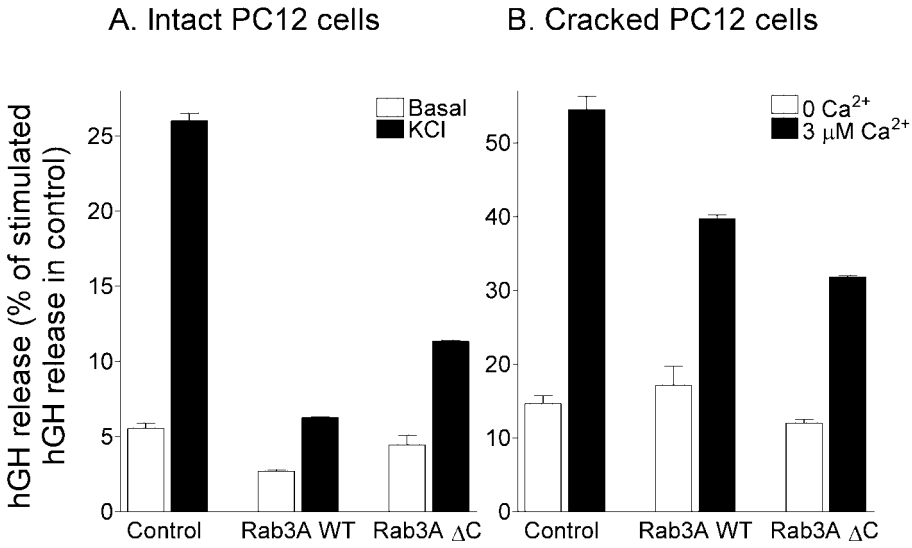

FIG. 7. **Comparison of the effect of transfected Rab3A on Ca^{2+}-stimulated exocytosis in intact PC12 cells (*A*) or cracked PC12 cells (*B*).** PC12 cells were co-transfected with the hGH vector and a control vector or expression vectors for full-length Rab3A or truncated Rab3A that lacks the C-terminal cysteines, which are geranylgeranylated (*Rab3AΔC*). Half of the transfected cells were analyzed intact using a 15-min KCl stimulation of secretion. The other half was "cracked" by freezing and thawing. Exocytosis of hGH-containing docked granules was stimulated by Ca^{2+} for 20 min in the presence of rat brain cytosol and Mg^{2+}-ATP. Data are from a single representative experiment performed in duplicate and are normalized to the control condition. Generally, cracked PC12 cells exhibit Ca^{2+}-independent and -dependent hGH release rates, respectively, of 10–15 and 45–50% total hGH/20 min.

in intact transfected PC12 cells than in cracked transfected PC12 cells (Fig. 7) suggests that the transfected protein may impair the biogenesis or disposition of secretory granules. To address this possibility, we expressed either hGH alone or hGH and Rab3A in transfected PC12 cells and then labeled dense core vesicles in the cells with [^{3}H]norepinephrine. The cells were then lysed and subfractionated on a sucrose gradient. Each fraction was analyzed by scintillation counting for [^{3}H]-norepinephrine, by radioimmunoassay for hGH, and by immunoblotting for synaptic proteins (Fig. 10). The results revealed that Rab3A, synaptotagmin 1, and SNARE proteins co-migrated in two major peaks on the gradient, the second of which coincided with the peak of [^{3}H]norepinephrine and hGH. Synaptophysin, on the other hand, was much more abundant on the first peak. These characteristics suggest that the first peak corresponds to synaptic-like microvesicles, which are enriched in synaptophysin, whereas the second peak corresponds to large dense core vesicles (50, 51). In Rab3A-transfected cells, the size of the second peak containing hGH is decreased but not shifted, whereas the norepinephrine peak (which serves as an internal control for vesicles derived from nontransfected cells in the same population) is unchanged. This observation indicates that Rab3A transfection may inhibit production of hGH, slow down the biogenesis of dense core vesicles, or promote the nonregulated exocytosis leading to a secondary loss of the vesicles.

To differentiate between these three possibilities, we first measured the total content of hGH produced in transfected cells as a function of co-transfection with wild type or mutant Rab3A. Transfection of wild type or GTP-fixed Rab3A decreased the hGH content ~4-fold (Fig. 11). Some reduction, however, is expected from co-transfection of another protein with hGH alone because any co-expression of another protein with hGH dilutes the transcription and translation factors and thus decreases the amount of hGH produced. Indeed, in transfected PC12 cells expressing GDP-fixed Rab3A (which does not inhibit Ca^{2+}-triggered exocytosis; see Fig. 9), the hGH levels are decreased 2-fold compared with controls (Fig. 11). Viewed in this light, the decrease in the hGH levels in the Rab3A transfected PC12 cells is not as great, suggesting that approximately half of the hGH is lost compared with the GDP form. However, loss of hGH in the large, dense core vesicle fraction (Fig. 10) appears to be more severe than the overall decrease of hGH in the cells (Fig. 11), indicating that it is not the biosynthesis of hGH but either its packaging into vesicles or the regulation of secretion that is impaired.

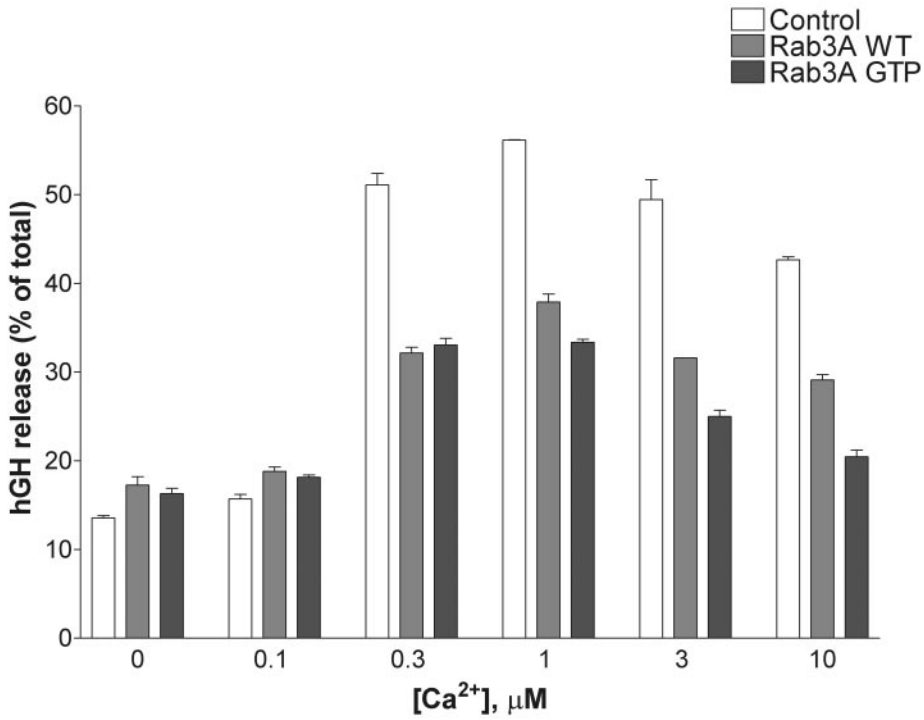

FIG. 8. **Effect of wild type and GTP-fixed Rab3A on Ca^{2+}-concentration dependence of hGH secretion from cracked PC12 cells.** PC12 cells co-transfected with a control vector or with vectors expressing wild type and GTP-fixed Rab3A were cracked as described in the legend to Fig. 7. Secretion of hGH was stimulated by the addition of Ca^{2+} at the indicated concentrations. Data shown are means ± S.E. from a single representative experiment performed in duplicate and repeated three times with similar results.

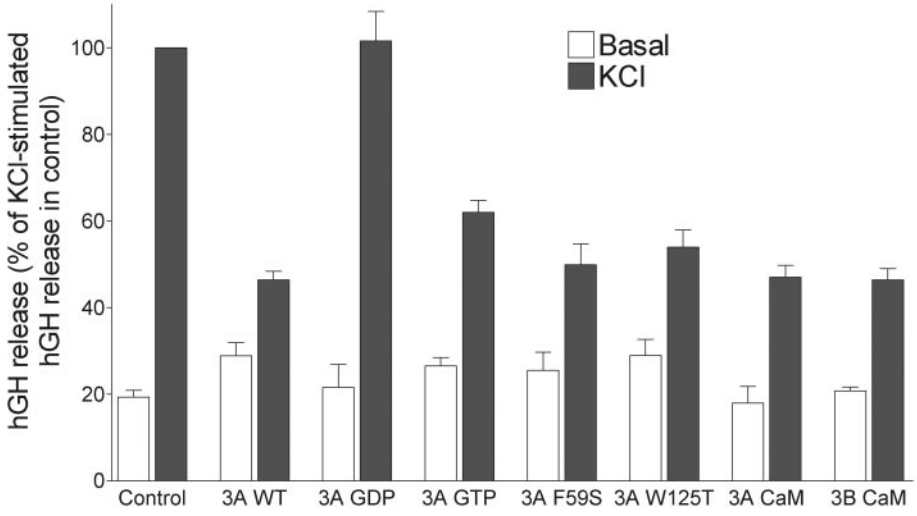

FIG. 9. **Effect of wild type and mutant Rab3 proteins on regulated exocytosis in PC12 cells.** PC12 cells were co-transfected with the hGH expression vector and either a control vector without an insert or various Rab3 expression vectors. Exocytosis was then stimulated from intact cells with 56 mM KCl as described in the legend to Fig. 6. Expression vectors encoded wild type Rab3A (*3A WT*); Rab3A mutants Q81L and T36N, which fix it in the GTP- and GDP-bound forms (*3A GTP* and *3A GDP*, respectively); Rab3A point mutants F59S and W125T, which interfere with interactions with the putative effectors RIM and rabphilin; and Rab3A and Rab3B double mutant R66L/R70T, referred to as "*3B CaM*" because it abolishes binding of Rab3s to calmodulin. Data shown are means ± S.E. of normalized results from three independent experiments performed in duplicate.

To test why Rab3A overexpression reduced the hGH content of the transfected cells, we measured the amount of hGH that is constitutively secreted from co-transfected cells. Fig. 12 shows that co-transfection of wild type Rab3A or mutant Rab3A that is permanently GTP-bound dramatically increased the amount of hGH that was secreted into the medium. In contrast, the GDP-fixed form of Rab3A had no effect compared with controls (Fig. 12). Because the same Rab3 proteins that increased constitutive secretion of hGH decreased the total cellular content of hGH (Fig. 11), the transfected Rab3 proteins must act by increasing the spontaneous, Ca^{2+}-independent secretion of hGH. An enhancement of constitutive exocytosis was also observed after transfection of Rab3B, Rab3C, and Rab3D, suggesting that the general inhibition of exocytosis by overexpressed wild type Rab3 proteins correlates with a general activation of constitutive exocytosis (data not shown).

DISCUSSION

Rab3A, Rab3B, Rab3C, and Rab3D together form a family of closely related GTP-binding proteins that interact with the same putative effectors but have been associated with divergent localizations and functions. One persistent problem is that these proteins have rarely been compared directly in the same experiment. In addition, most studies did not examine endogenous proteins but probed the localizations or effects of transfected proteins. Of the many questions arising from previous work on Rab3 proteins, the present work was designed to address two related, potentially important issues. First, do different Rab3 proteins have distinct or similar localizations and functions? Second, are the discrepancies between the proposed functions of Rab3 proteins, especially Rab3A, due to differences in the approaches? For example, the relatively weak phenotype of the Rab3A knock-out mice could reflect redundancy among Rab3 proteins, whereas the strong effects of Rab3A in transfected cells could be an indirect consequence of a secondary process. We have addressed these questions using antibodies standardized with recombinant proteins, to examine the relative expression and localization of the four Rab3 proteins, and transfected PC12 cells, to probe the functions of

TABLE I

Rab3 proteins expressed in PC12 cells by co-transfection with hGH to study the mechanism of Rab3-dependent inhibition of exocytosis

Rab3 Protein	Presumptive effect of mutations[a]	Effect on regulated exocytosis[b]	Effect on constitutive exocytosis[c]
Rab3A	Wild type	Strong inhibition	Activation
Rab3AΔC	Deletes C-terminal cysteines; thus not geranylgeranylated	Strong inhibition	ND
Rab3A-T36N	Inhibits GDP dissociation; thus preferentially GDP-bound	No inhibition	No effect
Rab3A-Q81L	Inhibits GTP hydrolysis; thus preferentially GTP-bound	Strong inhibition	Activation
Rab3A-F59S	Inhibits GTP-dependent rabphilin binding	Strong inhibition	ND
Rab3A-W125T	Highly conserved Rab3-specific residue	Strong inhibition	ND
Rab3A-R66L/R70T	Inhibits calmodulin binding	Strong inhibition	ND
Rab3B	Wild type	Strong inhibition	ND
Rab3B-Q81L	Inhibits GTP hydrolysis; thus preferentially GTP-bound	Strong inhibition	ND
Rab3B-R66L/R70T	Inhibits calmodulin binding	Strong inhibition	ND
Rab3C	Wild type	Strong inhibition	ND
Rab3C-Q89L	Inhibits GTP hydrolysis; thus preferentially GTP-bound	Strong inhibition	ND
Rab3D	Wild type	Strong inhibition	ND
Rab3D-Q81L	Inhibits GTP hydrolysis; thus preferentially GTP-bound	Strong inhibition	ND

[a] Based on Refs. 14 and 48.
[b] Effect on KCl-, ±-latrotoxin-, and Ca^{2+}-triggered release of co-transfected hGH as shown in Figs. 6–9.
[c] See Figs. 10–12. ND, not determined.

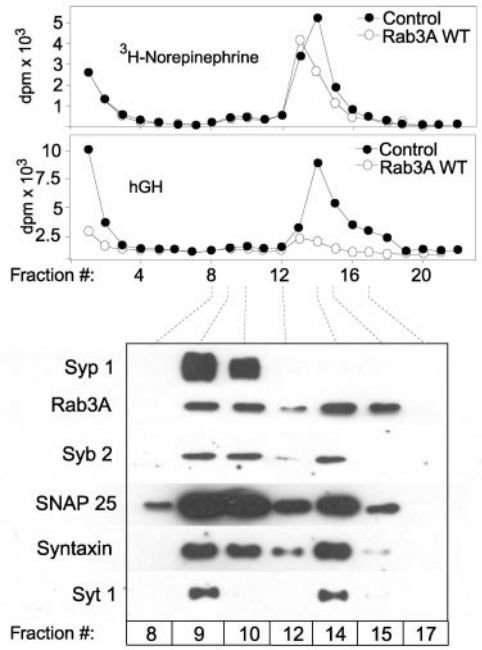

FIG. 10. **Subcellular localization of hGH in mock and Rab3A-transfected PC12 cells.** PC12 cells were co-transfected with hGH and control vector or Rab3A expression vector. Three days after transfection, cells were labeled overnight with [^{3}H]norepinephrine and lysed, and organelles in the postnuclear supernatants were separated on discontinuous sucrose gradients. Gradient fractions were analyzed by scintillation counting to measure [^{3}H]norepinephrine, by radioimmunoassay to measure hGH, and by immunoblotting for synaptophysin 1 (*Syp 1*), Rab3A, synaptobrevin 2 (*Syb 2*), SNAP-25, syntaxin 1, and synaptotagmin 1 (*Syt 1*) as indicated. Note that the [^{3}H]norepinephrine distribution reflects all PC12 cells, whereas the hGH distribution reflects only the small percentage of cells (<5%) that are transfected.

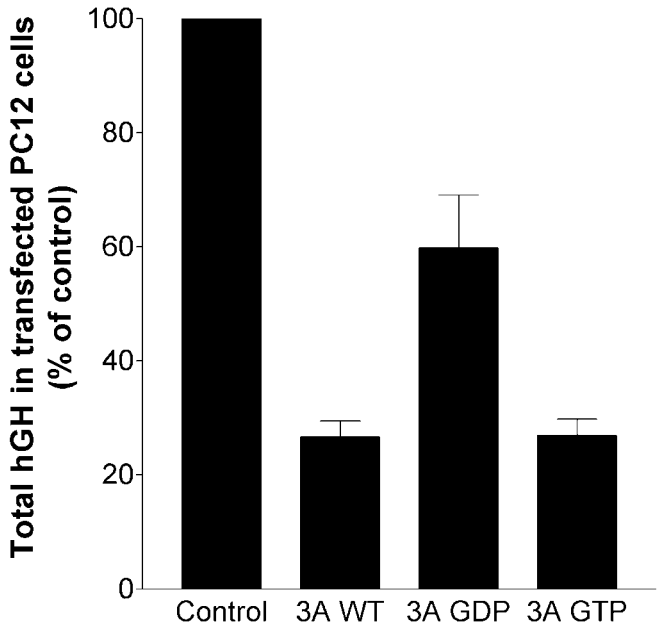

FIG. 11. **Effect of transfection of wild type and mutant Rab3A proteins on total cellular hGH levels.** PC12 cells were co-transfected with the hGH expression vector and with either control or test expression vectors as described in Fig. 8, and the total cellular levels of hGH were determined in resting cells. hGH levels are normalized to control values. Data shown are means ± S.E. from five independent experiments.

Rab3 proteins. Our results suggest the following conclusions.

1. Rab3A, Rab3B, and Rab3C are expressed primarily in the brain and endocrine cells, whereas Rab3D is synthesized in a different pattern with the highest levels in exocrine cells and adipose tissue. These results extend previous data (6, 7, 12, 43) by quantifying the concentrations of various Rab3 proteins. As a result, we show for example that the concentration of Rab3D in the lachrymal and parotid glands is twice that of Rab3A in the brain (where Rab3A is the most abundant Rab protein (2)) and that most tissues do not express detectable levels of any Rab3 protein (Fig. 2). The latter point is particularly important because the presence of significant mRNA levels for some Rab3 forms in the lung, liver, kidney, and testis suggested that these Rab3 proteins may play an important general role, despite the fact that no such role was detected in Rab3A knock-out mice. Clearly the mRNA levels provide only a first approximation to the place where a protein is actually expressed.

2. In the brain, Rab3A, Rab3B, and Rab3C are co-localized on synaptic vesicles but exhibit a differential distribution among brain regions (Figs. 3–5). Rab3A is uniformly present in all brain areas, Rab3B only in a subset of brain areas with the

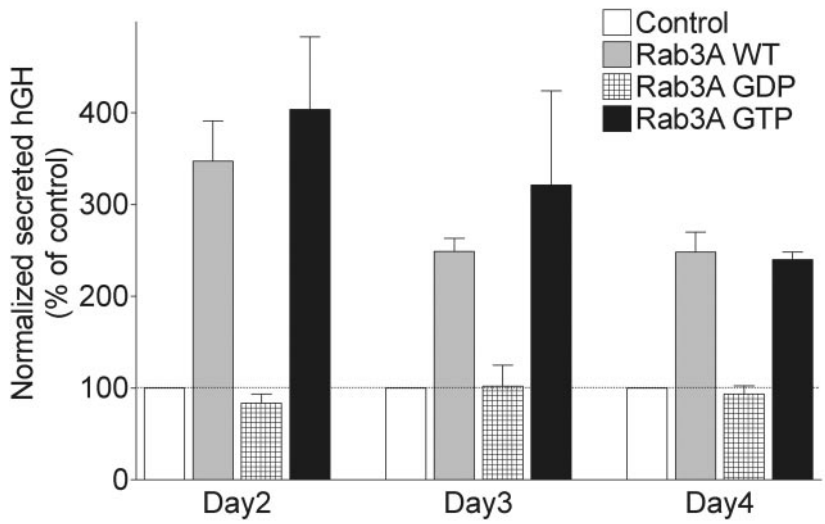

FIG. 12. **Effect of transfection of wild type and mutant Rab3A on constitutive secretion of hGH.** PC12 cells were co-transfected with the hGH expression vector and either control vector or expression vectors for wild type Rab3A and mutant Rab3A that were fixed in the GDP- and GTP-bound states, respectively. The amount of hGH in the extracellular medium was measured by radioimmunoassay on days 2, 3, and 4 after transfection and normalized to the amount of hGH remaining in the cells on day 4. Data are means ± S.E. from five independent experiments performed in triplicate.

highest levels in olfactory bulb, and Rab3C in most brain areas but at variable levels. This pattern is very similar to that observed for other synaptic vesicle proteins, for example synaptophysins, which are expressed in an ubiquitously (synaptophysin 1) and a variably distributed isoform (synaptophysin 2/synaptoporin; Ref. 29). Rab3D is also present in the brain, but its levels were too low to allow localization.

3. In transfected PC12 cells, all Rab3 proteins are dominant inhibitors as long as they bind GTP, but all effector interactions tested with specific mutants are dispensable for inhibition (Figs. 6–9; see also Ref. 14). Furthermore, the strong inhibition observed in intact cells is reduced in cracked cells, indicating that the inhibition does not operate by blocking a terminal step in Ca^{2+}-triggered exocytosis (Fig. 7). This conclusion is supported by the fact that the inhibition cannot be "rescued" by increases in Ca^{2+}-concentrations in the permeabilized cells (Fig. 8). A major limitation of these observations is that they were obtained in transfected PC12 cells; this does not prove that endogenous Rab3 proteins are similarly active, an issue that needs to be resolved using knock-out mice.

4. Finally, overexpression of wild type Rab3A or a Rab3A mutant that is permanently GTP-bound activates constitutive secretion of co-transfected hGH, leading to a decrease in the amount of remaining cellular hGH (Figs. 10–12). This result demonstrates that Rab3A may not actually inhibit secretion directly but rather may deplete the transfected cells of dense core vesicle content by allowing continuous exocytosis of their cargo. In this regard, Rab3 proteins are similar to Rab11b, which we recently found to be the only Rab protein tested among multiple such proteins that inhibited exocytosis.[2]

Overall, the available data reported in this and other studies (12, 14, 20) indicate that Rab3A, Rab3B, Rab3C, and Rab3D are functionally comparable based on similar localizations, a high degree of sequence homology, and equivalent inhibition of exocytosis in transfected PC12 cells. Clearly there are major differences in the cells and tissues that express the different Rab3 isoforms and possibly also in the functions of Rab3 proteins, because the biogenesis and fusion of secretory vesicles in exocrine glands containing Rab3D exhibit quite different properties from the biogenesis and fusion of endocrine and neuronal secretory vesicles. On the other hand, the high levels of "exocrine" Rab3D in the endocrine adenohypophysis (Fig. 3*B*) support the notion that Rab3 proteins function similarly in exocrine and endocrine exocytosis.

[2] M. Khvotchev and T. C. Südhof, manuscript in preparation.

The most important finding of our study may have been the observation that Rab3A overexpression in PC12 cells activates constitutive exocytosis, causing an apparent inhibition of Ca^{2+}-triggered exocytosis by depleting the pool of available hGH. This observation potentially explains contradictory results in the literature. It suggests that overexpressed GTP- but not GDP-bound Rab3A can circumvent the Ca^{2+}-control of exocytosis. The observation that Ca^{2+} acts in the final stage of exocytosis, which was also identified in the Rab3A knock-out as the point where the function of Rab3A becomes apparent, reconciles the knock-out data and the PC12 cell transfection data. This observation also suggests the reason that a decrease in the number of total and docked vesicles was observed in transfected PC12 cells expressing Rab3A and 3D (20). Although viewed together, the results reported here and previously argue for a general role of Rab3 proteins in the final stage of exocytosis, the mechanism involved is still unclear. Nevertheless, with the emerging convergence of the PC12 cell and knock-out data, it may now be possible to address this mechanism in further transfection experiments.

Acknowledgments—We thank I. Leznicki, A. Roth, Y. Tannhäuser, and E. Borowicz for technical assistance, S. Takamori for help with the synaptic vesicle purification by controlled-pore glass chromatography, W. Antonin for help with the immunoprecipitation experiments of synaptic vesicles, F. Benseler for help with the PCR cloning of the murine Rab3 isoforms, and H. Lodish for providing the mouse Rab3D cDNA clone.

REFERENCES

1. Fischer von Mollard, G., Mignery, G. A., Baumert, M., Perin, M. S., Hanson, T. J., Burger, P. M., Jahn, R., and Südhof, T. C. (1990) *Proc. Natl. Acad. Sci. U. S. A.* **87**, 1988–1992
2. Geppert, M., Bolshakov, V. Y., Siegelbaum, S. A., Takei, K., De Camilli, P., Hammer, R. E., and Südhof, T. C. (1994) *Nature* **369,** 493–497
3. Fischer von Mollard, G., Südhof, T. C., and Jahn, R. A. (1991) *Nature* **349,** 79–81
4. Fischer von Mollard, G., Stahl, B., Khoklatchev, A., Südhof, T. C., and Jahn, R. (1994) *J. Biol. Chem.* **269,** 10971–10974
5. Valentijn, J. A., Sengupta, D., Gumkowski, F. D., Tang, L. H., Konieczko, E. M., and Jamieson, J. D. (1996) *Eur. J. Cell Biol.* **70,** 33–41
6. Tuvim, M. J., Adachi, R., Chocano, J. F., Moore, R. H., Lampert, R. M., Zera, E., Romero, E., Knoll, B. J., and Dickey, B. F. (1999) *Am. J. Respir. Cell Mol. Biol.* **20,** 79–89
7. Ohnishi, H., Ernst, S. A., Wys, N., McNiven, M., and Williams, J. A. (1996) *Am. J. Physiol.* **271,** G531–G538
8. Lledo, P. M., Vernier, P., Vincent, J. D., Mason, W. T., and Zorec, R. (1993) *Nature* **364,** 540–544
9. Stettler, O., Nothias, F., Tavitian, B., and Vernier, P. (1995) *Eur. J. Neurosci.* **7,** 702–713
10. Lin, C. G., Lin, Y. C., Liu, H. W., and Kao, L. S. (1997) *Biochem. J.* **324,** 85–90
11. Baldini, G., Scherer, P. E., and Lodish, H. F. (1995) *Proc. Natl. Acad. Sci. U. S. A.* **92,** 4284–4288
12. Piiper, A., Leser, J., Lutz, M. P., Beil, M., and Zeuzem, S. (2001) *Biochem.*

Biophys. Res. Commun. **287,** 746–751
13. Weber, E., Jilling, T., and Kirk, K. L. (1996) *J. Biol. Chem.* **271,** 6963–6971
14. Chung, S. H., Joberty, G., Gelino, E. A., Macara, I. G., and Holz, R. W. (1999) *J. Biol. Chem.* **274,** 18113–18120
15. Iezzi, M., Escher, G., Meda, P., Charollais, A., Baldini, G., Darchen, F., Wollheim, C. B., and Regazzi, R. (1999) *Endocrinology* **13,** 202–212
16. Geppert, M., Goda, Y., Stevens, C., and Südhof, T. C. (1997) *Nature* **387,** 810–814
17. Castillo, P. E., Janz, R., Südhof, T. C., Malenka, R. C., and Nicoll, R. A. (1997) *Nature* **388,** 590–593
18. Holz, R. W., Brondyk, W. H., Senter, R. A., Kuizon, L., and Macara, I. G. (1994) *J. Biol. Chem.* **269,** 10229–10234
19. Johannes, L., Lledo, P. M., Roa, M., Vincent, J. D., Henry, J. P, and Darchen, F. (1994) *EMBO J.* **13,** 2029–2037
20. Martelli, A. M., Baldini, G., Tabellini, G., Koticha, D., Bareggi, R., and Baldini, G. (2000) *Traffic* **1,** 976–986
21. Johnston, P. A., Jahn, R., and Südhof, T. C. (1989) *J. Biol. Chem.* **264,** 1268–1273
22. Matteoli, M. Takei, K., Cameron, R., Hurlbut, P., Johnston, P. A., Südhof, T. C., Jahn, R., and De Camilli, P. (1991) *J. Cell Biol.* **115,** 625–633
23. Fischer von Mollard, G., Stahl, B., Walch-Solimena, C., Takei, K., Daniels, L., Khoklatchev, A., De Camilli, P., Südhof, T. C., and Jahn, R. (1994) *Eur. J. Cell Biol.* **65,** 319–326
24. Edelmann, L., Hanson, P. I., Chapman, E. R., and Jahn R. (1995) *EMBO J.* **14,** 224–231
25. Brose, N., Huntley, G. W., Stern-Bach, Y., Sharma, G., Morrison, J. H., and Heinemann, S. F. (1994) *J. Biol. Chem.* **269,** 16780–16784
26. Jahn, R., Schiebler, W., Ouimet, C., and Greengard, P. (1985) *Proc. Natl. Acad. Sci. U. S. A.* **82,** 4137–4141
27. Fasshauer, D., Antonin, W., Margittai, M., Pabst, S., and Jahn, R. (1999) *J. Biol. Chem.* **274,** 15440–15446
28. Li, C., Takei, K., Geppert, M., Daniell, L., Stenius, K., Chapman, E. R., Jahn, R., De Camilli, P., and Südhof, T. C. (1994) *Neuron* **13,** 885–898
29. Fykse, E. M., Takei, K., Walch-Solimena, C., Geppert, M., Jahn, R., De Camilli, P., and Südhof, T. C. (1993) *J. Neurosci.* **13,** 4997–5007
30. Laemmli, U. K. (1970) *Nature* **277,** 680–685
31. Towbin, H., Staehelin, T., and Gordon, J. (1979) *Proc. Natl. Acad. Sci. U. S. A.* **76,** 4350–4354
32. Schlüter, O. M., Schnell, E., Verhage, M., Tzounopoulos, T., Nicoll, R. A., Janz, R., Malenka, R. C., Geppert, M., and Südhof, T. C. (1999) *J. Neurosci.* **19,** 5834–5846
33. Bordier, C. (1981) *J. Biol. Chem.* **256,** 1604–1607
34. Mandell, J. W., Townes-Anderson, E., Czernik, A. J., Cameron, R., Greengard, P., and De Camilli, P. (1990) *Neuron* **5,** 19–33
35. Klenchin, V. A., Kowalshyk, J. A., and Martin, T. F. J. (1998) *Methods Companion Methods Enzymol.* **18,** 204–208
36. Nagy, A., Baker, R. R., Morris, S. J., and Whittaker, V. P. (1976) *Brain Res.* **109,** 285–309
37. Burger, P. M., Mehl, E., Cameron, P. L., Maycox, P. R., Baumert, M., Lottspeich, F., De Camilli, P., and Jahn, R. (1989) *Neuron* **3,** 715–720
38. Antonin, W., Holroyd, C., Fasshauer, D., Pabst, S., Von Mollard, G. F., and Jahn, R. A. (2000) *EMBO J.* **19,** 6453–6464
39. Matsui, Y., Kikuchi, A., Kondo, J., Hishida, T., Teranishi, Y., and Takai, Y. (1988) *J. Biol. Chem.* **263,** 11071–11074
40. Baumert, M., Fischer von Mollard, G. Jahn, R., and Südhof, T. C. (1993) *Biochem. J.* **293,** 157–163
41. Johnston, P. A., Archer, B. T. III, Robinson, K., Mignery, G. A., Jahn, R., and Südhof, T. C. (1991) *Neuron* **7,** 101–109
42. Farnsworth, C. C., Kawata, M., Yoshida, Y., Takai, Y., Gelb, M. H., and Glomset, J. A. (1991) *Proc. Natl. Acad. Sci. U. S. A.* **88,** 6196–6200
43. Baldini, G., Hohl, T., Lin, H. Y., and Lodish, H. F. (1992) *Proc. Natl. Acad. Sci. U. S. A.* **89,** 5049–5052
44. Ward, C. R., Faundes, D., and Foster, J. A. (1999) *Mol. Reprod. Dev.* **53,** 413–421
45. Yunes, R., Michaut, M., Tomes, C., and Mayorga, L. S. (2000) *Biol. Reprod.* **62,** 1084–1089
46. Südhof, T. C. (2001) *Annu. Rev. Neurosci.* **24,** 933–962
47. Sugita, S., Han, W., Butz, S., Liu, X., Fernandez-Chacon, R., Lao, Y., and Südhof, T. C. (2001) *Neuron* **30,** 459–473
48. Coppola, T., Perret-Menoud, V., Lüthi, S., Farnsworth, C. C., Glomset, J. A., and Regazzi, R. (1999) *EMBO J.* **18,** 5885–5891
49. Sugita, S., Shin, O.-H., Han, W., Lao, Y., and Südhof, T. C. (2002) *EMBO J.* **21,** 270–280
50. Johnston, P. A., Cameron, P. L., Stukenbrok, H., Jahn, R., De Camilli, P., and Südhof, T. C. (1989) *EMBO J.* **8,** 2863–2872
51. Clift-O'Grady, L., Linstedt, A. D., Lowe, A. W., Grote, E., and Kelly, R. B. (1990) *J. Cell Biol.* **110,** 1693–1703
52. Takamori, S., Riedel, D., and Jahn, R. (2000) *J. Neurosci* **20,** 4904–4911

MEMBRANE TRANSPORT STRUCTURE FUNCTION AND BIOGENESIS:

Localization *Versus* Function of Rab3 Proteins: EVIDENCE FOR A COMMON REGULATORY ROLE IN CONTROLLING FUSION

Oliver M. Schlüter, Mikhail Khvotchev, Reinhard Jahn and Thomas C. Südhof

J. Biol. Chem. 2002, 277:40919-40929.
doi: 10.1074/jbc.M203704200 originally published online August 6, 2002